ACCOUNTS of chemical research

Article

pubs.acs.org/accounts

Comparative Study of Raman Spectroscopy in Graphene and MoS_2-type Transition Metal Dichalcogenides

Published as part of the Accounts of Chemical Research special issue "2D Nanomaterials beyond Graphene".

Marcos A. Pimenta,* Elena del Corro, Bruno R. Carvalho, Cristiano Fantini, and Leandro M. Malard

Departamento de Física, Universidade Federal de Minas Gerais (UFMG), Caixa Postal 702, Belo Horizonte, 30123-970 Minas Gerais, Brazil

CONSPECTUS: Raman spectroscopy is one of the most powerful experimental tools to study graphene, since it provides much useful information for sample characterization. In this Account, we show that this technique is also convenient to study other bidimensional materials beyond graphene, and we will focus on the semiconducting transition metal dichalcogenides (MX_2), specifically on MoS_2 and WS_2.

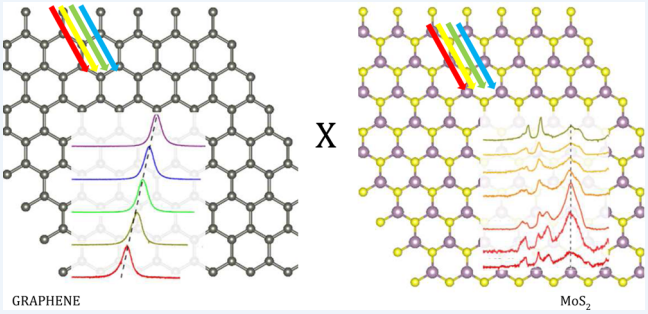

We start by comparing the atomic structure of graphene and 2H-MX_2 as a function of the number of layers in the sample. The first-order Raman active modes of each material can be predicted on the basis of their corresponding point-group symmetries. We show the analogies between graphene and 2H-MX_2 in their Raman spectra. Using several excitation wavelengths in the visible range, we analyze the first- and second-order features presented by each material. These are the E_{2g} and 2TO(K) bands in graphene (also known as the G and 2D bands, respectively) and the A_1', E′, and 2LA(M) bands in 2H MX_2. The double-resonance processes that originate the second-order bands are different for both systems, and we will discuss them in terms of the different electronic structure and phonon dispersion curves presented by each compound.

According to the electronic structure of graphene, which is a zero band gap semiconductor, the Raman spectrum is resonant for all the excitation wavelengths. Moreover, due to the linear behavior of the electronic dispersion near the K point, the double-resonance bands of graphene are dispersive, since their frequencies vary when we change the laser energy used for the sample excitation. In contrast, the semiconducting MX_2 materials present an excitonic resonance at the direct gap, and consequently, the double-resonance Raman bands of MX_2 are not dispersive, and only their intensities depend on the laser energy. In this sense, resonant Raman scattering experiments performed in transition metal dichalcogenides using a wide range of excitation energies can provide information about the electronic structure of these materials, which is complementary to other optical spectroscopies, such as absorption or photoluminescence.

Raman spectroscopy can also be useful to address disorder in MX_2 samples in a similar way as it is used in graphene. Both materials exhibit additional Raman features associated with phonons within the interior of the Brillouin zone that are activated by the presence of defects and that are not observed in pristine samples. Such is the case of the well-known D band of graphene. MX_2 samples present analogous features that are clearly observed at specific excitation energies. The origins of these double-resonance Raman bands in MX_2 are still subjects of current research. Finally, we discuss the suitability of Raman spectroscopy as a strain or doping sensor. Such applications of Raman spectroscopy are being extensively studied in the case of graphene, and considering its structural analogies with MX_2 systems, we show how this technique can also be used to provide strain/doping information for transition metal dichalcogenides.

INTRODUCTION

Raman spectroscopy has proven to be a very useful tool to study graphite-based materials, such as carbon nanotubes and graphene, and provides much different valuable information.[1−3] For example, the presence of disorder and defects manifests itself by the appearance of a disorder-induced Raman band, the so-called D band,[4] and this band can also be useful to distinguish between zigzag and armchair edges.[5] The phenomenom of charge transfer or doping by both electrons and holes is related to the change in the position and line width of the first-order Raman mode, the G band.[6] The G band splits into two components when the graphene sample is uniaxially strained,[7,8] and the strain value can be obtained from the splitting between these two components. The stacking order in graphite, crystalline or turbostratic, can also be distinguished from the shape of the 2D band (also called G′ band), which corresponds to a second-order Raman process involving two

Special Issue: 2D Nanomaterials beyond Graphene

Received: August 1, 2014
Published: December 9, 2014

DOI: 10.1021/ar500280m
Acc. Chem. Res. 2015, 48, 41−47

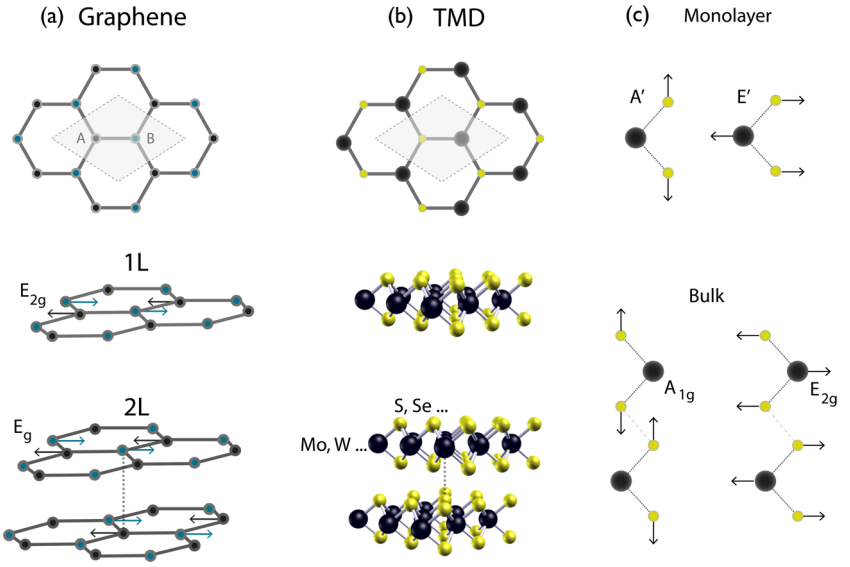

Figure 1. Atomic structure of (a) graphene/graphite and (b) monolayer TMD and bulk 2H-TMD. (c) Atomic displacements in two Raman active modes of monolayer TMD and bulk 2H-TMD.

phonons near the Dirac point with opposite momenta.[1] Both the D and 2D bands are enhanced by a special mechanism where there are, simultaneously, two or three resonances (double- or triple-resonance process).[9−11] The presence of a single atomic layer of graphene can be evidenced by the intensity ratio between the 2D and G bands ($I_{2D}/I_G > 1$) and the sharpness of the 2D band (fwhm around 25 cm^{-1}).[3,12] In the case of few-layer graphene stacked in the Bernal, also called the AB, configuration, the shape of the 2D band also provide information about the number of atomic layers.[12] Recently, it was shown that Raman spectroscopy is also extremely sensitive to the twisting angle in rotationally disordered bilayer graphene.[13,14]

All information on Raman spectroscopy discussed in the previous paragraph can be obtained using only one laser line. However, further valuable information can be obtained by changing the wavelength (or energy) of the laser. As we will discuss in the following, resonant Raman spectroscopy, where we analyze the intensity of the Raman peaks as a function of the laser energy, provides important information about electrons and their interaction with phonons.[2,15]

The transition metal dichalcogenides (TMDs) are layered compounds in which each layer has the basic form XMX (or MX_2), where M is a metal atom from the IVB, VB, and VIB columns in the periodic table and X is a chalcogen atom (S, Se, or Te). The electronic structure of these compounds depends on the transition metal species. The TMDs composed of a metal from groups IVB and VIB are semiconductors or insulators, and those composed of a metal from group VB atoms are metallic.[16] Although the bulk form of TMDs has been extensively studied in the past,[16] only recently monolayer and few-layer TMDs were obtained. In the case of semiconducting TMDs, they show a transition from an indirect band gap in the bulk to a direct gap for a monolayer.[17] This fact together with the rich physics of strong spin−orbit coupling in these materials has opened up several opportunities in both basic research and optoelectronic applications.[18]

In this Account, we will discuss the Raman spectra of bidimensional (2D) and bulk TMDs and compare these spectra with the graphene and graphite spectra. We will show the similarities and differences, and many possible ways to obtain physical information in these materials using Raman spectroscopy. We will present results in MoS_2 and WS_2 samples (monolayer and bulk) and discuss the origin and assignment of the Raman bands. The dependence of the TMD Raman spectra on the laser excitation energy will be discussed in terms of resonances with excitons. We will also give perspectives of new directions for Raman spectroscopy in TMDs that will be useful and will give much different information for these systems just as it also provides for graphene as a model system.

■ ATOMIC STRUCTURE OF GRAPHENE AND MX_2

Figure 1a shows the atomic structure for monolayer (1L) graphene. The unit cell contains two carbon atoms, A and B, each one forming a triangular 2D network but displaced from each other by the carbon−carbon distance. The structure of bulk crystalline graphite is also shown in Figure 1a and corresponds to a stacking of individual graphene layers in the direction perpendicular to the layer plane (*c*-axis) in an AB (or Bernal) stacking arrangement, in which the vacant centers of the hexagons in one layer have carbon atoms on hexagonal corner sites on the two adjacent graphene layers.[2]

In the case of MX_2, each layer corresponds to XMX triple atomic planes, with one plane of metal M atoms organized in a triangular lattice, and two planes of chalcogen atoms X, above and below the M atoms plane, also organized in triangular lattices. Depending on the arrangement of the X atoms, monolayer MX_2 appears in two distinct structures: the trigonal prismatic 2H (AbA) and the distorted octahedral 1T (AbC) arrangements. The 1T phase is metastable for MoS_2-type materials,[19] and therefore, we will only discuss in this Account the 2H TMD structure.

Figure 1b shows the atomic structure of a monolayer (1L) 2H-TMD, viewed perpendicularly and laterally to the basal plane.[16,20] Viewed from the top, the atomic structure looks similar to the single layer graphene structure, where the metal and chalcogen atoms would correspond, respectively, to the A and B carbon atoms in graphene. The unit cell is in this case composed of three atoms (one M and two X). The most common polytype of bulk MX_2 is the 2H-MX_2 structure where

DOI: 10.1021/ar500280m
Acc. Chem. Res. 2015, 48, 41−47

the TMD layers are stacked in a Bernal configuration, similarly to bulk crystalline graphite, as shown in Figure 1a,b.

Both Bernal stacked graphite and 2H-MX_2 crystalline structures belong to the $P6_3/mmc$ nonsymmorphic space group (D_{6h} point group),[16,21] with an inversion symmetry center in the middle of the two monolayers. The unit cells of graphite and bulk 2H-MX_2 structures are composed of four and six atoms, respectively. However, in the case of a monolayer, the symmetries of graphene and 2H-MX_2 are different: graphene belongs to the centrosymmetric point group D_{6h}, whereas MX_2 has no inversion symmetry and its point group is D_{3h}. In the case of bilayer MX_2 stacked in the Bernal configuration, the inversion symmetry operation is recovered, but due to the lack of translation symmetry along the z axis, the point group is D_{3d}. Therefore, the few layered TMD compounds with an even number of layers belong to the D_{3d} point group and those with an odd number of layers belong to the D_{3h} point group.

GROUP-THEORY ANALYSIS OF RAMAN MODES IN GRAPHENE AND 2H-MX_2

Monolayer graphene has only one first-order Raman active mode, belonging to the two-dimensional irreducible representation E_{2g}. It corresponds to the vibration of the sublattice formed by the A carbon atoms against the B carbon atom sublattice, in any direction of the basal plane, and gives rise to the so-called Raman G band, around 1580 cm^{-1}. In the case of bulk crystalline graphite, two modes are Raman active, both belonging to the E_{2g} representation. One of them appears at very low frequency (42 cm^{-1}) and corresponds to the rigid-layer mode, where two adjacent graphene layers vibrate against each other. In the high frequency mode, the atoms of each layer vibrate, like in the monolayer graphene E_{2g} mode.[2,3,21]

A single layer of 2H-MX_2 has three zone-center first-order Raman active modes belonging to the A_1', E′, and E″ irreducible representations of the D_{3h} group. For the A_1' mode, the metal atoms do not move and the chalcogen X atoms vibrate in the out-of-plane direction with the X atoms of the upper layer vibrating in-phase and against the lower layer of X atoms, as shown in Figure 1c. In the case of the E′ and E″ modes, the atomic displacements are in-plane. For the E′ mode, all X atoms move in-phase, and all M atoms move in-phase and in opposite directions. This mode, also shown in Figure 1c, is somewhat similar to the graphene Raman active mode (G band), where the A carbon atom sublattice vibrates against the B atom sublattice. For the E″ mode, the non-null elements of the Raman tensor correspond to the quadratic functions xz and yz. Therefore, this mode does not appear in the commonly used Raman backscattering configuration where the direction of the laser beam is perpendicular to the layer xy-plane. Therefore, the Raman spectra of monolayer 2H-MX_2 in this special backscattering configuration exhibit only two first-order Raman modes, with A_1' and E′ symmetries.[22]

The phonon dispersion relations for graphene and MoS_2 are shown in Figure 2a,b. The symmetries of the zone-center and Raman active modes are represented.[23] The eletronic structure of graphene (π electrons) and monolayer MoS_2 are shown in Figure 2c,d. While graphene is a zero gap semiconductor (the conduction and valence bands touch each other at the K and K′ points),[21] monolayer MoS_2 is a direct band gap semiconductor where the minimum of the conduction band and maxima of the valence band are at the K point.[17,24] The optical properties of

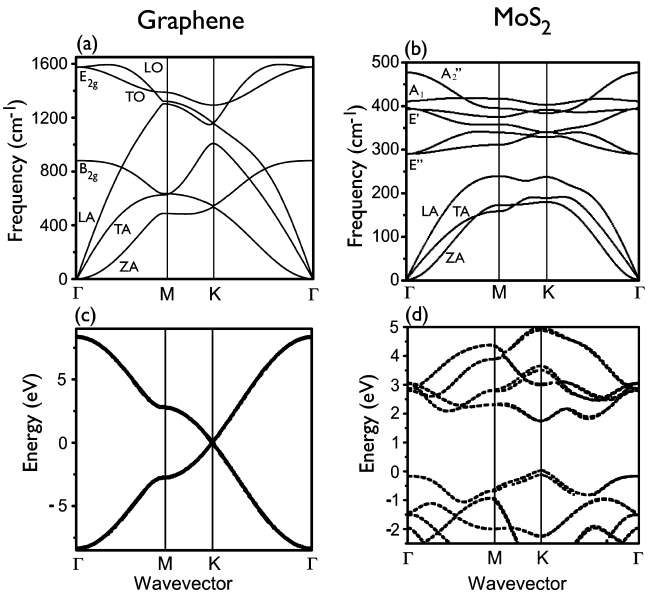

Figure 2. Phonon dispersion relations of (a) graphene and (b) MoS_2. Electronic structure of (c) graphene and (d) MoS_2.

MoS_2-type compounds are dominated by excitonic transitions at the K point of the Brillouin zone (BZ).[25]

For bulk 2H-MX_2, there are four Raman active modes, which are assigned according to the representations of the D_{6h} group as A_{1g}, E_{1g}, E^1_{2g}, and E^2_{2g}. The A_{1g}, E_{1g}, and E^1_{2g} modes correspond, respectively, to the A_1', E″, and E′ modes of monolayer MX_2, where the atoms in adjacent layers move in-phase with respect to inversion symmetry. The E^2_{2g} mode corresponds to the vibration of adjacent rigid layers with respect to each other, similar to the rigid-layer mode of graphite, and also appears at very low frequencies. Therefore, the Raman spectra of 2H-MX_2 crystals using conventional spectrometers and in a backscattering configuration discussed above, also exhibit only two first-order Raman peaks, with A_{1g} symmetry (out-of-plane atomic displacements) and E^1_{2g} symmetry (in-plane displacements).[26,27]

RESULTS AND DISCUSSION

Figure 3a shows the Raman spectrum of monolayer graphene. We can observe the so-called G band around 1580 cm^{-1}, which here we will call the E_{2g} band, since it corresponds to the zone-center Raman active mode with E_{2g} symmetry. Around 2700 cm^{-1}, we can observed a very strong peak, which is associated with two phonons of the iTO branch near the K point and which is called in the literature the 2D or G′ band. Since both denominations lack a precise physical meaning, we will call this feature here the 2TO(K) band. Notice that, despite the fact that this 2TO(K) band comes from a second-order process, it is usually more intense that the first-order E_{2g} band (G band) in monolayer graphene. Figure 3c shows the Raman spectrum of crystalline graphite, where we can see both the E_{2g} and 2TO(K) bands. Notice that the 2TO(K) band of graphite is weaker than the E_{2g} band and is clearly asymmetric, different from the case of monolayer graphene.[2,12]

It was proposed many years ago that the 2TO(K) band of graphitic systems is originated by a double-resonance (DR) Raman process, where two intermediate states of the Raman process are in resonance with real electronic states.[9,10] In this case, two of the terms in the denominator of the Raman

DOI: 10.1021/ar500280m
Acc. Chem. Res. 2015, 48, 41−47

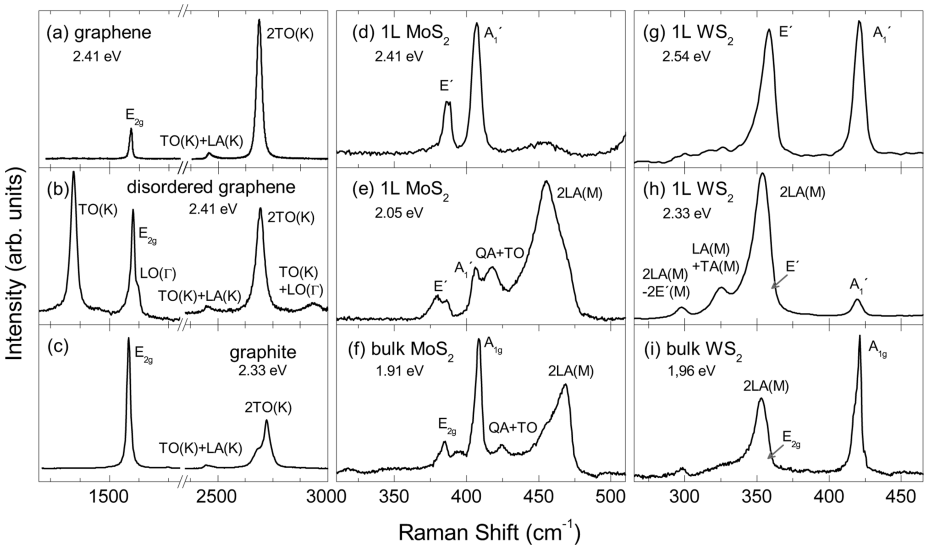

Figure 3. Raman spectra of (a) graphene, (b) disordered graphene, (c) graphite, (d, e) monolayer MoS_2 excited with different laser lines, (f) bulk MoS_2, (g, h) monolayer WS_2 excited with different laser lines, and (i) bulk WS_2. The different excitation energies (in eV) are represented. For graphene and graphite, the E_{2g}, TO(K), LO(Γ), and 2TO(K) bands corresponds, respectively, to the so-called G, D, D′, and 2D (or G′) bands.

intensity expression are simultaneously resonant, explaining why this second-order feature can be as intense as the first-order E_{2g} band. The fact that the 2TO(K) band can be even more intense than the E_{2g} band in monolayer graphene was ascribed to a triple-resonance (TR) Raman process, where all intermediate states of the Raman process, involving electrons and holes, are resonant.[11]

Figure 3b shows the Raman spectrum of a sample of disordered graphene. We can observe in this figure a strong feature around 1350 cm^{-1}, which is usually called the D-band, where the letter D stands for disorder (or defect). This band also comes from a DR process, but involving only one phonon of the iTO branch, near the K point. In this case, an elastic scattering process involving defects is needed for momentum conservation, and the presence of this band is a signature of defects or disorder in graphene systems. Since other Raman bands are also related to disorder or defects in graphene systems,[1] it is interesting to give a more precise notation for the D band, and we will call it here the TO(K) band. The origin of the other weak features in the Raman spectra of graphene systems is discussed in refs 1 and 2.

Let us now make a comparison between the Raman spectra of graphene and TMDs, discussing the similarities, the differences, and how the Raman spectra of TMDs provide useful information for these systems. Figure 3d,g shows the spectra of 1L MoS_2 and WS_2 recorded, respectively, with the 2.41 and 2.54 eV laser lines. The two prominent peaks in these figures correspond to the first-order Raman active modes with E′ and A_1' symmetries. The E′ mode is somewhat similar to the E_{2g} mode of graphene (G band), since it involves an in-plane vibration of the sublattice formed by metal atoms against the sublattices formed by the chalcogens. The A_1' mode of TMDs has no correspondence with graphene, since it corresponds to out-of-plane vibrations of the upper and lower sublattices of chalcogen atoms against each other.

Figure 3e,h shows the spectra of 1L MoS_2 and WS_2 recorded with different laser lines, with 2.05 and 2.33 eV energies, respectively. Notice that the Raman spectrum of TMDs is strongly dependent on laser energies, since the spectra in Figure 3e,h are completely different from those shown in Figure 3d,g. We can see now a number of features that are associated with second-order processes involving combinations (sums and differences) of phonons within the interior of the Brillouin zone (BZ). A detailed study of the second-order bands in MoS_2 and WS_2 can be found in refs 26 and 28−31. Here we will only focus on the most intense second-order feature, which involves two phonons of the longitudinal acoustic (LA) branch with opposite momenta, at the M point of the BZ. This band is, therefore, called the 2LA(M) band.[31] It is interesting to observe that the second-order 2LA(M) band is more intense than the first-order A_1 and E′ bands in Figure 3e,h, and this result is similar to the behavior of 1L graphene, where the 2TO(K) band is more intense than the first-order E_{2g} band (see Figure 3a).

The Raman spectra of bulk MoS_2 and WS_2 are shown, respectively, in Figure 3f,i. The positions and attribution of the Raman features are the same as 1L MoS_2 and WS_2, but now the 2LA(M) band is less intense than the first-order A_{1g} band. Notice that this behavior is similar to crystalline graphite, where the 2TO(K) band is less intense than the E_{2g} (see Figure 3c).

The fact that the 2LA(M) band can be stronger than the first-order bands in 1L TMDs suggests that the second-order spectra in TMDs also involve double- or triple-resonance processes, as in the case of graphene. In a recent study, the double-resonance process in TMDs was calculated using a fourth-order Fermi golden rule, and it was demonstrated that the intensity of the 2LA(M) band comes from a DR Raman process involving phonons at the M point of the BZ.[32] Many other weak peaks also comes from a combination of phonons at the M point.[29]

The essential check for the DR mechanism is a resonance Raman experiment, where the Raman spectra is studied as a function of the laser excitation energy. Figure 4a,b show the spectra of 1L graphene and MoS_2, respectively, recorded with different laser lines. In the graphene spectra, we only show the spectral region of the 2TO(K) band. Notice in Figure 4a that the 2TO(K) band is dispersive, its position depending linearly on the laser energy in the visible range. This behavior can be explained by the DR process in graphene, which is illustrated in Figure 4c.[2,3] Due to the linear dispersion of electrons in

DOI: 10.1021/ar500280m
Acc. Chem. Res. 2015, 48, 41−47

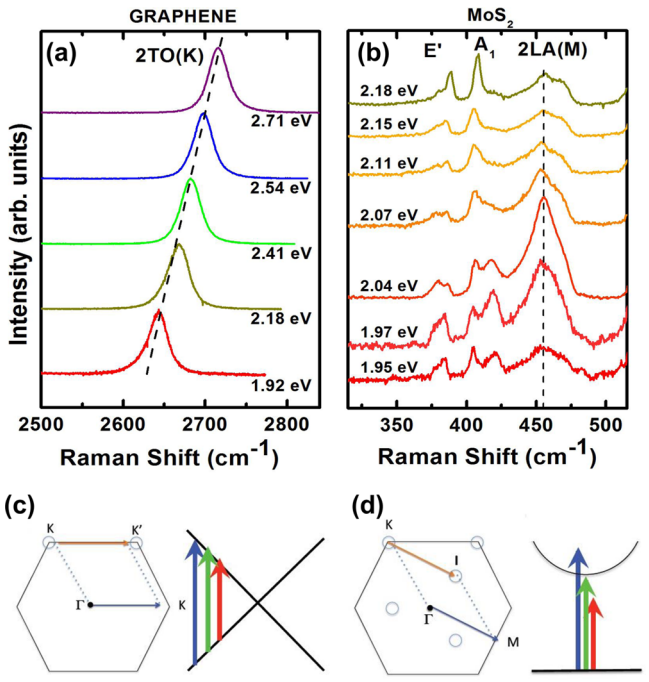

Figure 4. Dependence of the double-resonance bands of (a) graphene and (b) MoS_2 on the laser energies. Diagrams showing the directions of phonons involved with DR process and transitions with different energy photons in (c) graphene and (d) MoS_2-type TMDs.

graphene, the Raman process is always resonant, because the energy of the incident photon will always correspond to the separation between the conduction and valence band in a specific point in the BZ near the Dirac (or K) point (see Figure 4c). The 2TO(K) band is associated with an intervalley process, involving resonances with valleys around the K and K′ points. We can see in Figure 4c that the wavevector of the phonon conecting points around K and K′ is, in fact, close to the K point (compare the orange and blue horizontal arrows in the figure). Therefore, when the double- and triple-resonance processes that originate the 2TO(K) band are probed with different laser lines, phonons with different wavevectors around K are involved, and consequently the position of the 2TO(K) band changes and provides information about the dispersion of electrons and phonons in graphene systems.[2]

Figure 4b shows the Raman spectra of 1L MoS_2 recorded with different laser lines. Now we can observe that the 2LA(M) band is not dispersive, and only its intensity changes with varying laser energy. In particular, the 2LA(M) band is more intense for laser energies around 2 eV, which corresponds to the B exciton energy in 1L MoS_2,[25] suggesting that it is really associated with a double-resonance process. Resonance Raman scattering can provide useful information about the electronic states of these materials. For this reason, in the literature we can find a number of papers combining Raman characterization with other optical spectroscopies, such as photoluminescence.[33]

Figure 4d illustrates the proposed DR mechanism for TMDs.[32] It now involves resonances at valleys at the K and I points (the I point is the intermediate point between Γ and K). It is shown in this figure that the phonon that connects these two valleys has a wavevector at the M point (compare the orange and blue arrows in the BZ). The optical spectrum of TMD systems of the MoS_2 family is dominated by excitonic transitions involving electronic states at the K point.[25] A resonant process with excitonic states is illustrated in Figure 4d. Notice that the double-resonance mechanism will enhance the intensity of 2(LA) bands only in a small range of energies that are in close resonance with the exciton states at the K point and the intermediate state at the I point. Therefore, the process involving resonances with excitonic transitions in TMDs explains our observed results shown in Figure 4b, where the intensity of the 2LA(M) band, and not its frequency, depends on the laser energy.

Let us now discuss the possibility of using Raman spectroscopy to characterize disorder and defects in TMDs. In the case of graphene, a number of features in the spectrum are activated by disorder, and the stronger one (the D band) is related to phonons belonging to the iTO branch near the K point. Therefore, this band might be called the TO(K) band.

It was reported many years ago that disorder-induced Raman bands also appear in the spectrum of MoS_2 and WS_2 films, around 223 and 176 cm^{-1}, respectively,[34] and their frequencies correspond to the frequencies of the phonon of the LA branch at the M point in MoS_2 and WS_2. Therefore, we call this disorder-induced feature the LA(M) band. This band might be also associated with a DR process illustrated in Figure 4d, involving one phonon and a defect for momentum conservation, in contrast to the 2LA(M) band that involves two phonons. So, the behavior of the LA(M) and 2LA(M) bands in TMDs seems to be analogous to the TO(K) (or D) and 2TO(K) (or 2D) bands in graphene. The observation of other weak peaks induced by disorder were also reported for MoS_2 and WS_2.[35] These bands involve phonons of other branches within the interior of the BZ in TMDs that are activated by disorder, showing that Raman spectroscopy is also very useful to characterize disorder and defects in these systems.

Raman spectroscopy is also a very useful tool to distinguish between monolayer or few-layer graphene and bulk graphite, both from the shape and intensity of the 2TO(K) band[2,12] and from the appearance of new bands associated with interlayer breathing and shear vibrations.[36] Few-layer TMDs can also be characterized by Raman spectroscopy. For example in MoS_2, it has been shown that the splitting between the A_1' and E′ band frequencies is related to the number of layers.[37] It was shown recently that extra first-order Raman modes that are absent in both 1L and bulk are activated in the spectra of few-layer TMDs.[22] These new modes belong the totally symmetric irreducible representation and involve out-of-plane vibrations of the M and X atoms.

The presence of external charges and doping in graphene can also be characterized from the position and line width of the first-order E_{2g} band.[6,38] Moderate doping of graphene systems, with both electrons and holes, stiffens and narrows the E_{2g} band, due to the suppression of the electron−phonon mechanism that gives rise to the Kohn anomaly. This effect reveals the nonadiabatic behavior of electron−phonon interaction in graphene.[2,3] In a recent study of a monolayer MoS_2 transistor,[39] it was shown that the A_1' mode softens and broadens with electron doping, whereas the E′ Raman mode remains essentially inert. This observation shows that TMD devices exhibit an opposite behavior compared with graphene, and this behavior is ascribed to the fact that they are semiconductors and phonon renormalization occurs within the adiabatic approximation.[39] Raman spectroscopy may also be useful to identify doping of TMD systems with other type of atoms, such as MoS_2 doped with Se.[40]

DOI: 10.1021/ar500280m
Acc. Chem. Res. 2015, 48, 41−47

Finally, let us discuss the possibility of using Raman spectroscopy to characterize strain in 2D systems. As discussed in the last section, the first-order E_{2g} Raman mode in graphene is a double-degenerate mode that involves vibration of the sublattices formed by the A and B carbon atoms against each other. Due to the hexagonal symmetry of the graphene structure, the frequency does not depend on the vibration direction in the *xy*-plane. However, when graphene is uniaxially strained, the degeneracy is broken, and the E_{2g} band splits into two components (E^{+}_{2g} and E^{-}_{2g}), which are associated with vibrations parallel and perpendicular to the strain direction.[8,41] The splitting between these two components can be used as a strain gauge.

The E′ mode in 1L TMD (or the E^{1}_{2g} mode in bulk TMDs) is analogous to the E_{2g} mode in graphene. It is also a double-degenerate mode involving the in-plane vibration of the M and X sublattices against each other in any direction in the *xy*-plane. The splitting of the E′ (or E^{1}_{2g}) is also expected to occur in uniaxially strained TMDs. For MoS_2, it was observed as a frequency shift of the E′ mode as a function of applied strain.[42] However, according to our knowledge, the expected splitting of the E′ (or E^{1}_{2g}) mode into two components in strained TMDs was not yet observed, and further experiments are needed to confirm this prediction.

CONCLUSIONS

In this Account we made a comparative study of Raman spectroscopy in graphene and TMD systems of the MoS_2 family. We first discussed the analogies and differences of the atomic structures, phonon dispersion, and electronic structures, and we presented a group theory analysis of the first-order Raman modes in 1L and bulk systems. The double-resonance processes in graphene and TMDs were compared, showing that they involve phonons in different points within the BZ. The double-resonance bands in graphene are dispersive, due to the linear behavior of the electronic dispersion near the K point, whereas in the case of TMDs, they are not dispersive and only the intensities depend on the laser energy, in agreement with a double-resonance process in TMDs involving excitonic transitions. We showed that in analogy to the disorder-induced D band in graphene, new Raman features associated with phonons within the interior of the BZ in TMDs are activated by disorder (or defects), showing that Raman spectroscopy is also useful to characterize disorder in these systems. We have briefly mentioned that Raman spectroscopy is useful to characterize and distinguish few-layer TMDs, and finally, we also showed that this technique can also be used to provide information about doping and strain in TMDs.

METHODS AND EXPERIMENTAL DETAILS

The graphene and 1L MoS_2 samples were obtained by mechanical exfoliation of natural graphite and 2H-MoS_2 crystals transferred to a Si substrate with a 300 nm thick SiO_2 coating. The 1L WS_2 samples consist of CVD growth triangular islands synthesized as described elsewhere.[32] The micro-Raman measurements were registered in a DILOR XY triple-monochromator spectrometer equipped with N_2-cooled charge-couple device (CCD) detectors and with 1800 g/mm diffraction gratings, giving spectral resolution better than 1 cm^{-1}. The graphene and WS_2 samples were excited by an Ar/Kr ion laser with excitation energies of 1.92, 2.18, 2.41, 2.54, and 2.71 eV. Additionally, the MoS_2 sample was excited by a tunable dye laser (with DCM Special and rhodamine 6G dyes), covering a wide excitation energies from 1.90 to 2.15 eV. All the measurements were conducted in backscattering geometry at room temperature. The samples were focused by a 100× objective providing a spot size of 2 μm in diameter. The laser power at the sample surface was kept below 1.0 mW in order to avoid sample heating.

AUTHOR INFORMATION

Corresponding Author

*E-mail: mpimenta@fisica.ufmg.br.

Funding

This work was supported by the Brazilian Institute of Science and Technology (INCT) in Carbon Nanomaterials and the Brazilian agencies CNPq, CAPES and FAPEMIG.

Notes

The authors declare no competing financial interest.

Biographies

Marcos A. Pimenta was born on April 11, 1958, in Belo Horizonte, Brazil, and received his Ph.D. in Physics from the University of Orleans, France. He became professor at the Department of Physics of the Universidade Federal de Minas Gerais (UFMG) in 1989, and in 1992, he implemented the Raman spectroscopy laboratory at UFMG. His research in the last years covered resonant Raman spectroscopy of carbon nanotubes, graphene, and other 2D materials..

Elena del Corro was born on February 5, 1982, in Madrid, Spain. She obtained a B.S. degree and a Ph.D. in Chemistry from the Complutense University of Madrid in 2011. She carried out a postdoctoral stay in the Department of Physics at UFMG before joining the Academy of Sciences of the Czech Republic as a postdoctoral researcher to study the electronic properties of strained graphene.

Bruno R. Carvalho was born on October 1, 1989, in Cuiabá, Brazil. He graduated in Physics at Universidade Federal de Mato Grosso in 2010, where he also received his Master degree in Physics in 2013. He is currently a Ph.D. student under the supervision of Prof. Dr. Marcos A. Pimenta at the UFMG. His doctoral research focuses on electronic and vibrational properties of 2D materials by Raman spectroscopy.

Cristiano Fantini was born on September 1, 1975, in Belo Horizonte, Brazil, and received his Ph.D. in Physics from the UFMG in 2005, working with resonant Raman spectroscopy in carbon nanotubes. In 2008, he became professor at the Physics Department at UFMG. His current research is focused in the optical properties of carbon nanotubes and two-dimensional materials.

Leandro M. Malard was born on January 28, 1982, in Belo Horizonte, Brazil, and received his Ph.D. in Physics from the UFMG, working with resonant Raman spectroscopy in graphene. In 2011, he became professor at the Physics Department at UFMG, and his current research is focused on the optical properties of two-dimensional materials, including time-resolved and nonlinear optics.

REFERENCES

(1) Pimenta, M. A.; Dresselhaus, G.; Dresselhaus, M. S.; Cancado, L. G.; Jorio, A.; Saito, R. Studying disorder in graphite-based systems by Raman spectroscopy. *Phys. Chem. Chem. Phys.* **2007**, *9*, 1276−1290.
(2) Malard, L.; Pimenta, M.; Dresselhaus, G.; Dresselhaus, M. Raman spectroscopy in graphene. *Phys. Rep.* **2009**, *473*, 51−87.

DOI: 10.1021/ar500280m
Acc. Chem. Res. 2015, 48, 41−47

(3) Ferrari, A. C.; Basko, D. M. Raman spectroscopy as a versatile tool for studying the properties of graphene. *Nat. Nanotechnol.* **2013**, *8*, 235−246.
(4) Tuinstra, F.; Koenig, J. L. Raman spectrum of graphite. *J. Chem. Phys.* **1970**, *53*, 1126−1130.
(5) Cançado, L. G.; Pimenta, M. A.; Neves, B. R. A.; Dantas, M. S. S.; Jorio, A. Influence of the atomic structure on the Raman spectra of graphite edges. *Phys. Rev. Lett.* **2004**, *93*, No. 247401.
(6) Das, A.; Pisana, S.; Chakraborty, B.; Piscanec, S.; Saha, S. K.; Waghmare, U. V.; Novoselov, K. S.; Krishnamurthy, H. R.; Geim, A. K.; Ferrari, A. C.; Sood, A. K. Monitoring dopants by Raman scattering in an electrochemically top-gated graphene transistor. *Nat. Nanotechnol.* **2008**, *3*, 210−215.
(7) Huang, M.; Yan, H.; Chen, C.; Song, D.; Heinz, T. F.; Hone, J. Phonon softening and crystallographic orientation of strained graphene studied by Raman spectroscopy. *Proc. Natl. Acad. Sci. USA* **2009**, *106*, 7304−7308.
(8) Mohiuddin, T. M. G.; Lombardo, A.; Nair, R. R.; Bonetti, A.; Savini, G.; Jalil, R.; Bonini, N.; Basko, D. M.; Galiotis, C.; Marzari, N.; Novoselov, K. S.; Geim, A. K.; Ferrari, A. C. Uniaxial strain in graphene by Raman spectroscopy: *G* peak splitting, Grüneisen parameters, and sample orientation. *Phys. Rev. B* **2009**, *79*, No. 205433.
(9) Baranov, A. V.; Bekhterev, A. N.; Bobovich, Y. S.; Petrov, V. I. Interpretation of certain characteristics in Raman spectra of graphite and glassy carbon. *Opt. Spectrosk.* **1987**, *62*, 1036−1042.
(10) Thomsen, C.; Reich, S. Double resonant Raman scattering in graphite. *Phys. Rev. Lett.* **2000**, *85*, 5214−5217.
(11) Venezuela, P.; Lazzeri, M.; Mauri, F. Theory of double-resonant Raman spectra in graphene: Intensity and line shape of defect-induced and two-phonon bands. *Phys. Rev. B* **2011**, *84*, No. 035433.
(12) Ferrari, A. C.; Meyer, J. C.; Scardaci, V.; Casiraghi, C.; Lazzeri, M.; Mauri, F.; Piscanec, S.; Jiang, D.; Novoselov, K. S.; Roth, S.; Geim, A. K. Raman spectrum of graphene and graphene layers. *Phys. Rev. Lett.* **2006**, *97*, No. 187401.
(13) Havener, R. W.; Zhuang, H.; Brown, L.; Hennig, R. G.; Park, J. Angle-resolved Raman imaging of interlayer rotations and interactions in twisted bilayer graphene. *Nano Lett.* **2012**, *12*, 3162−3167.
(14) Kim, K.; Coh, S.; Tan, L. Z.; Regan, W.; Yuk, J. M.; Chatterjee, E.; Crommie, M. F.; Cohen, M. L.; Louie, S. G.; Zettl, A. Raman spectroscopy study of rotated double-layer graphene: Misorientation-angle dependence of electronic structure. *Phys. Rev. Lett.* **2012**, *108*, No. 246103.
(15) Malard, L. M.; Nilsson, J.; Elias, D. C.; Brant, J. C.; Plentz, F.; Alves, E. S.; Castro Neto, A. H.; Pimenta, M. A. Probing the electronic structure of bilayer graphene by Raman scattering. *Phys. Rev. B* **2007**, *76*, No. 201401.
(16) Wilson, J.; Yoffe, A. The transition metal dichalcogenides discussion and interpretation of the observed optical, electrical and structural properties. *Adv. Phys.* **1969**, *18*, 193−335.
(17) Mak, K. F.; Lee, C.; Hone, J.; Shan, J.; Heinz, T. F. Atomically thin MoS_2: A new direct-gap semiconductor. *Phys. Rev. Lett.* **2010**, *105*, No. 136805.
(18) Xu, X.; Yao, W.; Xiao, D.; Heinz, T. F. Spin and pseudospins in layered transition metal dichalcogenides. *Nat. Phys.* **2014**, *10*, 343−350.
(19) Wypych, F.; Schöllhorn, R. 1T-MoS_2, a new metallic modification of molybdenum disulfide. *J. Chem. Soc., Chem. Commun.* **1992**, 1386−1388.
(20) Ganatra, R.; Zhang, Q. Few-layer MoS_2: A promising layered semiconductor. *ACS Nano* **2014**, *8*, 4074−4099.
(21) Saito, R.; Dresselhaus, G.; Dresselhaus, M. *Physical Properties of Carbon Nanotubes*; Imperial College Press: London, 1998.
(22) Terrones, H.; Corro, E. D.; Feng, S.; Poumirol, J. M.; Rhodes, D.; Smirnov, D.; Pradhan, N. R.; Lin, Z.; Nguyen, M. A. T.; Elias, A. L.; Mallouk, T. E.; Balicas, L.; Pimenta, M. A.; Terrones, M. New first order Raman-active modes in few layered transition metal dichalcogenides. *Sci. Rep.* **2014**, *4*, No. 4215.
(23) Molina-Sánchez, A.; Wirtz, L. Phonons in single-layer and few-layer MoS_2 and WS_2. *Phys. Rev. B* **2011**, *84*, No. 155413.
(24) Splendiani, A.; Sun, L.; Zhang, Y.; Li, T.; Kim, J.; Chim, C.-Y.; Galli, G.; Wang, F. Emerging photoluminescence in monolayer MoS_2. *Nano Lett.* **2010**, *10*, 1271−1275.
(25) Qiu, D. Y.; da Jornada, F. H.; Louie, S. G. Optical spectrum of MoS_2: Many-body effects and diversity of exciton states. *Phys. Rev. Lett.* **2013**, *111*, No. 216805.
(26) Sekine, T.; Nakashizu, T.; Toyoda, K.; Uchinokura, K.; Matsuura, E. Raman scattering in layered compound 2H-WS_2. *Solid State Commun.* **1980**, *35*, 371−373.
(27) Sekine, T.; Izumi, M.; Nakashizu, T.; Uchinokura, K.; Matsuura, E. Raman scattering and infrared reflectance in 2H-$MoSe_2$. *J. Phys. Soc. Jpn.* **1980**, *49*, 1069−1077.
(28) Sourisseau, C.; Cruege, F.; Fouassier, M.; Alba, M. Second-order Raman effects, inelastic neutron scattering and lattice dynamics in 2H-WS_2. *Chem. Phys.* **1991**, *150*, 281−293.
(29) Golasa, K.; Grzeszczyk, M.; Leszczyński, P.; Faugeras, C.; Nicolet, A. A. L.; Wysmolek, A.; Potemski, M.; Babiński, A. Multiphonon resonant Raman scattering in MoS_2. *Appl. Phys. Lett.* **2014**, *104*, No. 092106.
(30) Stacy, A.; Hodul, D. Raman spectra of IVB and VIB transition metal disulfides using laser energies near the absorption edges. *J. Phys. Chem. Solids* **1985**, *46*, 405−409.
(31) Chen, J.; Wang, C. Second order Raman spectrum of MoS_2. *Solid State Commun.* **1974**, *14*, 857−860.
(32) Berkdemir, A.; Gutierrez, H. R.; Botello-Mendez, A. R.; Perea-Lopez, N.; Elias, A. L.; Chia, C.-I.; Wang, B.; Crespi, V. H.; Lopez-Urias, F.; Charlier, J.-C.; Terrones, H.; Terrones, M. Identification of individual and few layers of WS_2 using Raman spectroscopy. *Sci. Rep.* **2013**, *3*, 1755.
(33) del Corro, E.; Terrones, H.; Elias, A.; Fantini, C.; Feng, S.; Nguyen, M. A.; Mallouk, T. E.; Terrones, M.; Pimenta, M. A. Excited excitonic states in 1L, 2L, 3L, and bulk WSe_2 observed by resonant Raman spectroscopy. *ACS Nano* **2014**, *8*, 9629−9635.
(34) McDevitt, N. T.; Zabinski, J. S.; Donley, M. S.; Bultman, J. E. Disorder-induced low-frequency Raman band observed in deposited MoS_2 films. *Appl. Spectrosc.* **1994**, *48*, 733−736.
(35) Frey, G. L.; Tenne, R.; Matthews, M. J.; Dresselhaus, M. S.; Dresselhaus, G. Raman and resonance Raman investigation of MoS_2 nanoparticles. *Phys. Rev. B* **1999**, *60*, 2883.
(36) Lui, C. H.; Heinz, T. F. Measurement of layer breathing mode vibrations in few-layer graphene. *Phys. Rev. B* **2013**, *87*, No. 121404.
(37) Lee, C.; Yan, H.; Brus, L. E.; Heinz, T. F.; Hone, J.; Ryu, S. Anomalous lattice vibrations of single- and few-layer MoS_2. *ACS Nano* **2010**, *4*, 2695−2700.
(38) Yan, J.; Zhang, Y.; Kim, P.; Pinczuk, A. Electric field effect tuning of electron-phonon coupling in graphene. *Phys. Rev. Lett.* **2007**, *98*, No. 166802.
(39) Chakraborty, B.; Bera, A.; Muthu, D. V. S.; Bhowmick, S.; Waghmare, U. V.; Sood, A. K. Symmetry-dependent phonon renormalization in monolayer MoS_2 transistor. *Phys. Rev. B* **2012**, *85*, No. 161403.
(40) Gong, Y.; Liu, Z.; Lupini, A. R.; Shi, G.; Lin, J.; Najmaei, S.; Lin, Z.; Elias, A. L.; Berkdemir, A.; You, G.; Terrones, H.; Terrones, M.; Vajtai, R.; Pantelides, S. T.; Pennycook, S. J.; Lou, J.; Zhou, W.; Ajayan, P. M. Band gap engineering and layer-by-layer mapping of selenium-doped molybdenum disulfide. *Nano Lett.* **2014**, *14*, 442−449.
(41) Huang, M.; Yan, H.; Heinz, T. F.; Hone, J. Probing strain-induced electronic structure change in graphene by Raman spectroscopy. *Nano Lett.* **2010**, *10*, 4074−4079.
(42) Rice, C.; Young, R. J.; Zan, R.; Bangert, U.; Wolverson, D.; Georgiou, T.; Jalil, R.; Novoselov, K. S. Raman-scattering measurements and first-principles calculations of strain-induced phonon shifts in monolayer MoS_2. *Phys. Rev. B* **2013**, *87*, No. 081307.

DOI: 10.1021/ar500280m
Acc. Chem. Res. 2015, 48, 41−47